King's College London

# Complex Energy Landscapes: Sherrington-Kirkpatrick Model vs P-Spin Glass Spherical Model

Supervisor: Prof. Reimer Kuhn

Author: Sufyan Ali

$15^{th}$ September 2022

# Contents

**Abstract**

This study concerns the comparative analysis of the energy landscapes between the Sherrington–Kirkpatrick model and the spherical p-spin glass model, through the implementation of the 'Optimisation by move-class deflation' algorithm using the Python programming language. The problem of finding the ground state energies is tackled, the nature of the metastable states are investigated and is compared for the two models. Since the 'Optimisation by move-class deflation' algorithm is sensitive to the topology of the two model's complex energy landscape, thus the algorithm is used as a diagnostic tool for comparison between the two models.

# 1 Introduction

Spin glass systems are characterised by frustration and quenched disorder. To provide intuition for the frustration found in spin glass systems, consider a 2-D magnetic system with three magnetic dipoles (spins), with orientations 'up' or 'down', residing on the corners of a triangle, with couplings $J_{ij} : i, j \in \{1, 2, 3\}$ such that $\prod_{\langle i,j \rangle} J_{ij} < 0$, where $\langle i, j \rangle$ implies the product is run over all pairs of $(i, j)$. The free energy is minimised, and thus the magnetic system is stable, when all spins are oriented according to their coupling type. However for this magnetic system, once two of the spins align according to their coupling type, the third one is frustrated because its two possible configurations cannot minimise the free energy whilst simultaneously satisfying their coupling type with both of the other two, hence the magnetic system is frustrated since it fluctuates between the two possible configurations. Since this effect occurs for each spin, the ground state is sixfold degenerate. Spin glasses are magnetic systems that have an approximately

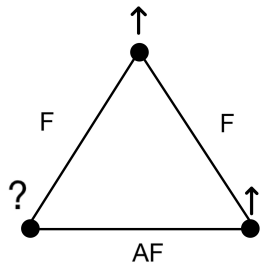


Figure 1: Illustration of a simple frustrated 2-D magnetic system. Bonds marked "F" correspond to ferromagnetic interaction and "AF" correspond to an antiferromagnetic interaction. One possible coupling type and spin orientations at the corner sites is shown.

equal a priori probability of having ferromagnetic or antiferromagnetic couplings between the spins [10]. Therefore as with the previous example provided, spin glass systems have the property of displaying fluctuations between many metastable states (frustration) which yields a 'rugged' (complex) energy landscape. Furthermore, the interactions between the magnetic dipoles are random variables which do not evolve with time, therefore the competition between exchange interactions does not lead to a long range ordering of the magnetic moments, but rather to an almost random freezing of their distribution (quenched disorder). Spin glass systems are a prominent field of study in disordered state physics, which have lead to many developments in mathematical techniques such as 'replica symmetry breaking' (RSB) developed by Giorgio Parisi, however the applications of the research into spin glass systems are extensive, and are found in diverse areas such as combinatorial optimisation [7], neural networks [4, 12], econophysics[11] and protein folding[5].

The Edwards-Anderson (EA) model was the first model developed in modern theory of spin glass systems in 1975 [1]. Edwards and Anderson essentially argued that reductionist approaches are not essential to analyse spin glass systems, and that the essential physics of the spin glass systems is in the competition of the ferromagnetic and antiferromagnetic interactions, implying that studying the Hamiltonian should be sufficient to derive and predict tangible and meaningful macroscopic features. The EA model models magnetic systems with spins arranged on a $D$-dimensional lattice with only nearest neighbor (n.n) interactions. The Hamiltonian of the EA model of size $N$ ($N$ spins) is given by,

$$H(\boldsymbol{\sigma}) = \sum_{\langle i,j \rangle_{\text{n.n}}} J_{ij}\sigma_i\sigma_j \tag{1}$$

where $i$ is a point on the $D$-dimensional lattice, $\langle i, j \rangle_{\text{n.n}}$ implies the sum is run over the nearest neighbours of the points on the $D$-dimensional lattice, the nearest neighbour coupling given by $J_{ij} \sim N(J_0, J^2/N)$ and the vector of spins denoted by $\boldsymbol{\sigma} = (\sigma_i) : \sigma_i \in \{-1, +1\}$, yielding $2^N$ number of spin configurations,

each lying on the N-dimensional hyper-cube. Later within that same year, Sherrington and Kirkpatrick (SK) had developed a model of magnetic systems that was an extension of the EA model that encompasses long range interactions, assumes the infinite volume limit and does not assume a particular geometric structure of the magnetic system [2]. This study investigates the SK model with the Hamiltonian for a system of size $N$ given by,

$$H_N(\boldsymbol{\sigma}) = -\sum_{<i,j>} J_{ij}\sigma_i\sigma_j \tag{2}$$

where $< i, j >$ implies the sum is run over every distinct pair-wise combinations of the $N$ spins, with the coupling set as $J_{ij} \sim N(0, 1/N)\ \forall\ i \neq j : i, j \in \Sigma = \{1, 2, 3, ..., N\}$, and $\boldsymbol{\sigma} = (\sigma_i)_{i\in\Sigma} : \sigma_i \in \{-1, +1\}$. A generalisation of the SK model is the $p$-spin glass spherical model which considers $p$-spin interactions instead of pair-wise interactions, where $p \leq N$. Along with the SK model, this study also investigates the $p$-spin glass spherical model, for the case of $p = 3$, with the Hamiltonian for a system of size $N$ given by,

$$H_N(\boldsymbol{\sigma}) = -\sum_{1\leq i_1\leq i_2,...,\leq i_p\leq N} J_{i_1,i_2,...,i_p}\sigma_{i_1}\sigma_{i_2}\cdots\sigma_{i_p} \tag{3}$$

with the couplings set as $J_{i_1,i_2,...,i_p} \sim N(0, p!/(2N^{p-1}))$, $\sigma_i \in \mathbb{R} : |\boldsymbol{\sigma}|^2 = N$, yielding the points on the surface of an $N$-dimensional hyper-sphere of radius $\sqrt{N}$ as the set of possible spin configurations.

There is the problem of finding these ground state energies, which is considered to be an N-P hard, and have been tackled through the use of various algorithms to obtain numerical results of the ground state energies [7, 8, 3]. This study aims to use the Optimisation by move-class deflation (OMCD) algorithm [9] to present qualitative differences between the complex energy landscapes of the SK model and the p-spin glass spherical model for $p = 3$ (most prominently studied form of the p-spin glass spherical model). The study begins with a comparison of the ground state energies of the two models, given in Sect.3. To provide a comparison of the metastable states at zero temperature dynamics between both models, the study proceeds on to investigate the probability distribution of the overlap between the ground state spin configurations over many replicas, along with the absolute difference in the ground state energies between the replicas, for a given bond configuration, found in Sect.4. Since OMCD is sensitive to the topology of the complex energy landscapes of spin glass systems, as explained in [9], OMCD is used to provide a phase-space diagnostics, given in Sect.5. The summary and discussion of the results are given in Sect.6

## 2 Heuristics of the OMCD Algorithm

This study implements the OMCD algorithm for a system size, denoted by $N$, by first initialising a random spin configuration and bond configuration, thus calculates the energy (initial energy) corresponding to the initial spin configuration. Denote the move-class schedule by the set $\mathcal{D} = \{d_0, d_0 - 1, d_0 - 2, ..., 1\}$, where $d \in \mathcal{D}$ denotes the move-class size which the OMCD algorithm systematically takes values in $\mathcal{D}$ in descending order, hence $d_0$ denotes the initial move-class size. For each $d$, the algorithm performs 'moves' on $d$ randomly chosen spins simultaneously, with the number of attempted moves (time-steps), denoted by $t_d$, such that,

$$t_d = t_{mcs} \cdot \text{int}(N/d) \tag{4}$$

where $t_{mcs}$ denotes the number of Monte Carlo steps (mcs), equivalently the number of time-steps per spin, which is kept constant $\forall\ d \in \mathcal{D}$ and for each mcs, the algorithm performs $\text{int}(N/d)$ moves, where '*int()*' is the Python function that returns the integer portion of the argument, therefore the number of attempted moves per move-class $d$ increases as $d$ decreases. For the SK model, a 'move' performed on each of the $d$ spins is given by: $\sigma_i^{\text{new}} \to -\sigma_i^{\text{old}}$. For the p-spin glass spherical model, a 'move' performed on each of the $d$ spins is given by: $\sigma_i^{\text{new}} \to \sigma_i^{\text{old}} + \delta s : \delta s \sim N(0, 1)$, followed by a scaling of the new vector of spins: $\boldsymbol{\sigma}^{\text{new}} \to \sqrt{N} \cdot \boldsymbol{\sigma}^{\text{new}}/|\boldsymbol{\sigma}^{\text{new}}|$, so that the new vector of spins satisfies the spherical constraint. The

modification to the 'flip' procedure for the p-spin glass spherical model is made since if the 'flips' are performed just like they are for the SK model, this results in $\sigma_{i\in\Sigma}^{\text{new}} \in \{+\sigma_{i\in\Sigma}^{\text{initial}}, -\sigma_{i\in\Sigma}^{\text{initial}}\}$, hence a given $\boldsymbol{\sigma}^{\text{initial}}$ strictly determines $2^N$ subsequent possible $\boldsymbol{\sigma}^{\text{new}}$. Hence this modification reduces the bias of $\boldsymbol{\sigma}^{\text{initial}}$ on the set of possible $\boldsymbol{\sigma}^{\text{new}}$, thus allowing for a more rich exploration of the complex energy landscape. The condition for an accepted move is $H(\boldsymbol{\sigma_{new}}) \leq H(\boldsymbol{\sigma_{old}})$, thus moves at $d = 1$ correspond to zero temperature Glauber dynamics, hence OMCD may be used to obtain ground state energies of the SK model and the p-spin glass spherical model.

## 3 Ground State Energies

In attempt to find good ground state energies of the two model's using the OMCD algorithm, one is left with possible choices for the $d_0$ to be used for each system size, typically $1 << d_0 << N$. Since the energy barriers for the SK model scale with $N$, and if the energy landscape of the p-spin glass spherical model is similar to the SK model, this should manifest through OMCD when trying to find good ground state energies for both models with the existence of an optimal $d_0$, $d_{0optimal}$. For both the SK model and the p-spin glass spherical model, the free energy for the system size $N$, $F_N(\beta)$, is given by,

$$F_N(\beta) = \frac{1}{N}\mathbb{E}[\log Z_N(\beta)] : Z_N(\beta) = \sum_{\{\boldsymbol{\sigma}\}} e^{\beta H_N(\boldsymbol{\sigma})} \tag{5}$$

$$\therefore E_{gs}^N = \lim_{\beta\to\infty} \frac{F_N(\beta)}{\beta} \tag{6}$$

$$\therefore E_{gs}^N = \frac{1}{N}\mathbb{E}[H_N(\boldsymbol{\sigma})] : \boldsymbol{\sigma} \in \{\boldsymbol{\sigma}\}_{gs} \tag{7}$$

where $\beta = 1/T$, with $T$ denoting the temperature of the system. In addition, $E_{gs}^N$ denotes the ground state energy of the system (of size $N$) and $\{\boldsymbol{\sigma}\}_{gs}$ denotes the set of spin configurations that exist at the ground state. Using the notation $E_{gs} = \lim_{N\to\infty}[E_{gs}^N]$, work done by G.Parisi in [3] show that for the SK model, $E_{gs} = 0.7633 \pm 10^{-4}$ and work done by J. Kurchan, G.Parisi and M.A. Virasoro in [6] show that for the p-spin glass spherical model, by minimising the TAP equations at zero temperature, $E_{gs} = -\sqrt{2(p-1)/p}$, therefore for $p = 3$, $E_{gs} = -1.1547$.

Therefore proceeding to find good ground state energies, OMCD runs are performed for multiple $d_0$, and for each $d_0$, $I_N$ OMCD runs are performed per $M_N$ bond configurations. For each bond configuration, $E_{min} = \inf\{E_{final}^{\alpha} : \alpha = [1, 2, 3..., I_N]\}$, where $E_{final}^{\alpha}$ denotes the final energy obtained in the $\alpha^{th}$ OMCD run, the results of $\langle E_{min}\rangle$ as a function of $d_0$ are presented in Figs.2,3,4,5. The approximation of the ground state energies by OMCD is denoted by $E_{\text{gs}}^N = \langle E_{min}^N(d_{0optimal})\rangle$, where $d_{0optimal} = \text{argmin}\{E_{min}^N(d_0)\}$, which is listed for both models in the tables 1 and 2 respectively. Thus the ground state energies for each model is obtained by extrapolating the fitting of $E_{\text{gs}}^N$ with $N$ given by the equation,

$$\langle E_{min}\rangle = a + bN^{-2/3} \tag{8}$$

$$\langle E_{min}\rangle = a + bN^{-5/8} \tag{9}$$

for the SK model and p-spin glass spherical model respectively. The plots of which, along with the model's respective values for $a$ and $b$, are given in Fig.6, with the value of $a$ corresponding to the approximation of the ground state energy. Therefore for the SK model $E_{gs}$ is approximated as -0.75946, yielding a statistical error equal to -0.00834. For the p-spin glass spherical model $E_{gs}$ is approximated as -1.14389, yielding a statistical error equal to -0.010811.

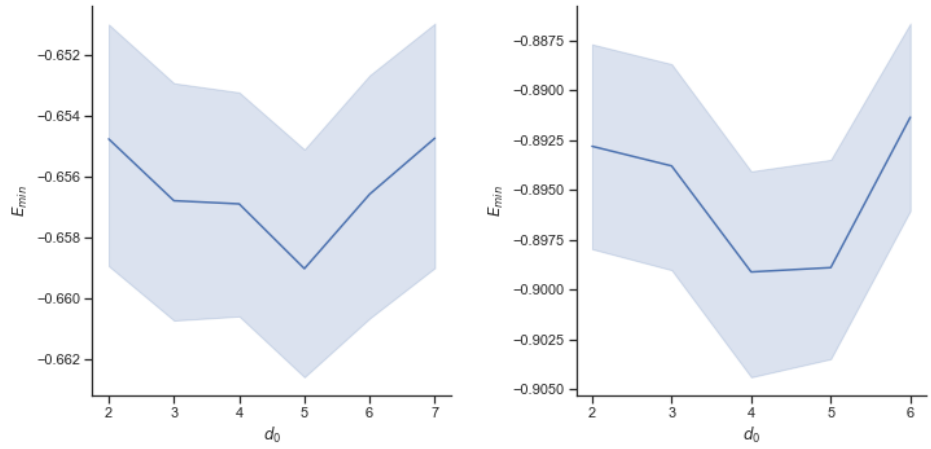


Figure 2: $E_{min}$, with the 95% confidence interval around $\langle E_{min} \rangle$, as a function of $d_0$ for $N = 20$. SK model (left): $t_{mcs} = 1000, I_N = 3, M_N = 1000$. P-spin glass spherical model (right):$t_{mcs} = 400, I_N = 3, M_N = 500$.

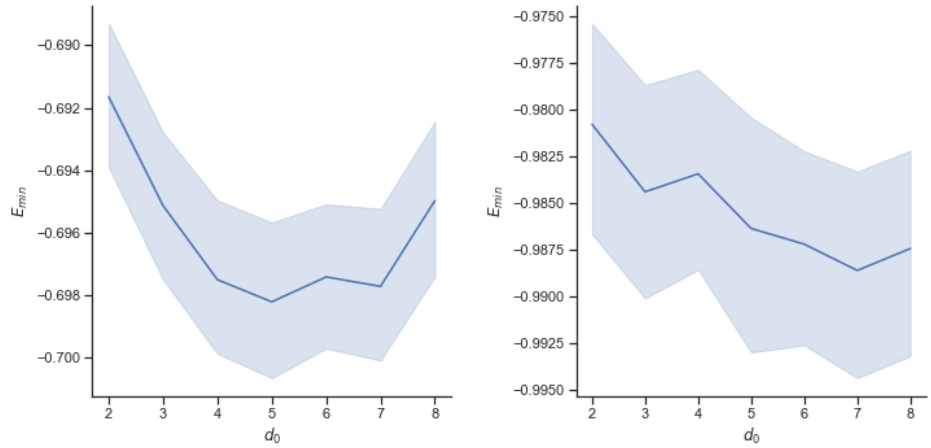


Figure 3: $E_{min}$, with the 95% confidence interval around $\langle E_{min} \rangle$, as a function of $d_0$ for $N = 40$. SK model (left): $t_{mcs} = 800, I_N = 5, M_N = 1000$. P-spin glass spherical model (right): $t_{mcs} = 200, I_N = 3, M_N = 1000$.

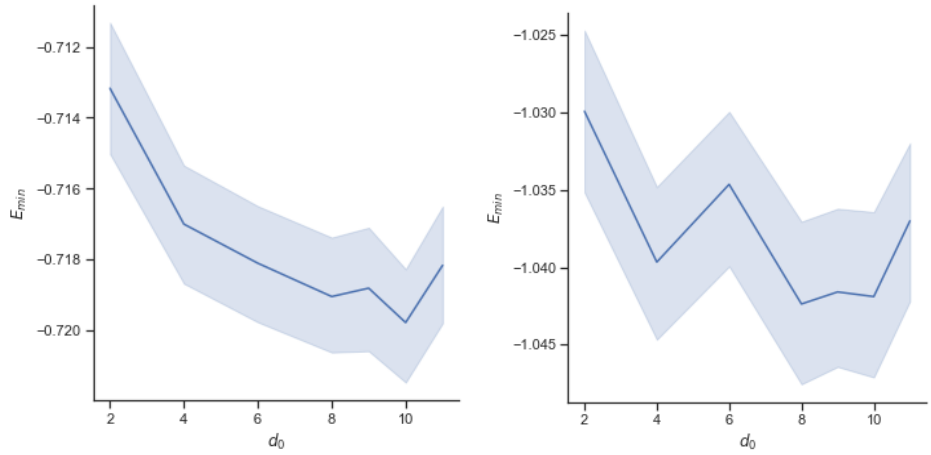


Figure 4: $E_{min}$, with the 95% confidence interval around $\langle E_{min} \rangle$, as a function of $d_0$ for $N = 80$. SK model (left): $t_{mcs} = 600, I_N = 7, M_N = 800$. p-spin glass spherical model (right): $t_{mcs} = 100, I_N = 5, M_N = 100$.

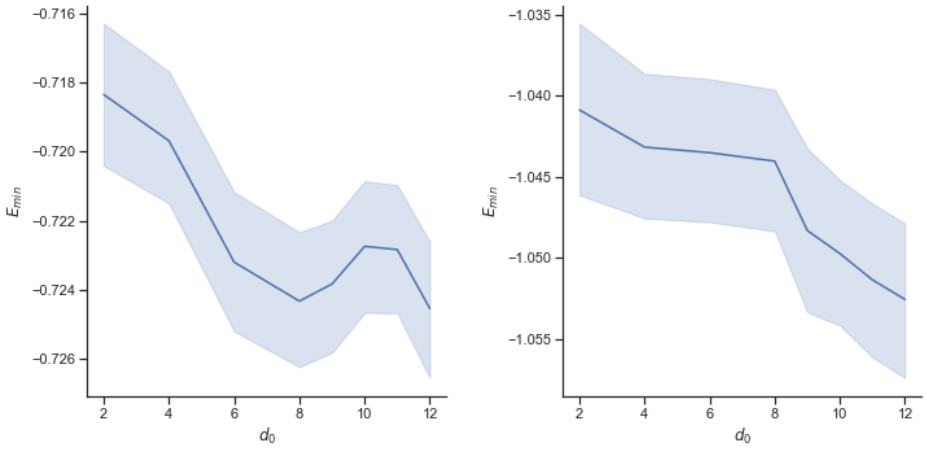


Figure 5: $E_{min}$, with the 95% confidence interval around $\langle E_{min} \rangle$, as a function of $d_0$ for $N = 100$. SK model (left): $t_{mcs} = 500, I_N = 8, M_N = 500$. P-spin glass spherical model (right): $t_{mcs} = 100, I_N = 5, M_N = 100$.

| $N$ | $d_{0optimal}$ | $\langle E_{min}(d_{0optimal}) \rangle$ | $\sigma(E_{min}(d_{0optimal}))$ |
|---|---|---|---|
| 20 | 5 | -0.65903 | 0.059858 |
| 40 | 5 | -0.69821 | 0.039198 |
| 80 | 10 | -0.71979 | 0.023816 |
| 100 | 12 | -0.72454 | 0.021211 |

Table 1: List of computational results, to approximate ground state energies for the SK model with their standard deviation and $d_{0optimal}$, for the respective system size $N$.

| $N$ | $d_{0optimal}$ | $\langle E_{min}(d_{0optimal}) \rangle$ | $\sigma(E_{min}(d_{0optimal}))$ |
|---|---|---|---|
| 20 | 4 | -0.89910 | 0.059077 |
| 40 | 7 | -0.98862 | 0.040464 |
| 80 | 8 | -1.0424 | 0.026790 |
| 100 | 12 | -1.0526 | 0.023839 |

Table 2: List of computational results, to approximate ground state energies for the p-spin glass spherical model with their standard deviation and $d_{0optimal}$, for the respective system size $N$.

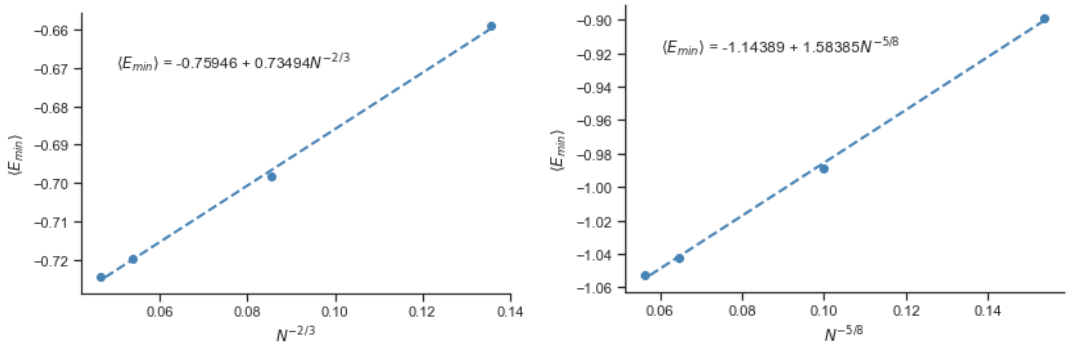


Figure 6: Linear fit of ground state energies obtained by OMCD for the SK model (left) and the p-spin glass spherical model (right) for $N = 20, 40, 80, 100$.

## 4 Overlap of Final Spin Configurations

As mentioned in the introduction, spin glass systems at a given temperature contain many metastable states between which they fluctuate. The existence of the many metastable spin configurations is captured by the overlap of the final spin configurations between many replicas of a given bond configuration, with the overlap of spin configurations between any two replicas, $\alpha, \beta$, defined by,

$$q(\boldsymbol{\sigma}^{\alpha}, \boldsymbol{\sigma}^{\beta}) = \frac{1}{N}\boldsymbol{\sigma}^{\alpha} \cdot \boldsymbol{\sigma}^{\beta} \tag{10}$$

which yields the bounds, $-1 \leq q(\boldsymbol{\sigma}^{\alpha}, \boldsymbol{\sigma}^{\beta}) \leq 1$. One can also verify the existence of the many metastable states by considering, in conjunction with the spin overlaps between many replicas, the absolute difference of their respective energies. The absolute difference between the final energies obtained between any two replicas $\alpha, \beta$ is defined by,

$$\mathcal{E}(\boldsymbol{\sigma}^{\alpha}, \boldsymbol{\sigma}^{\beta}) = |E_{min}(\boldsymbol{\sigma}^{\alpha}) - E_{min}(\boldsymbol{\sigma}^{\beta})| \tag{11}$$

which yields the obvious bound $\mathcal{E}(\boldsymbol{\sigma}^{\alpha}, \boldsymbol{\sigma}^{\beta}) \geq 0$. Since single spin moves are attempted for $d = 1$, which corresponds to zero–temperature Monte–Carlo dynamics, OMCD may be used to investigate the zero temperature dynamics of the SK model and the p-spin spherical glass model. Therefore for a sufficiently large enough $t_{mcs}$, the investigation into the nature of the metastable states at ground states can be conducted through the analysis of the final spin configurations and the final energies obtained by many OMCD runs for a given bond configuration, which is presented in Fig.7,8, 9,10. Again, assuming that the set $t_{mcs}$ parameter is sufficiently large for the algorithm to obtain good ground states of the respective system, as well as $I_N$ and $M_N$ being sufficiently large, most OMCD runs would obtain the same ground state energies and their respective metastable states, as is confirmed in the plots for both models.

Note that for the SK model, $H(\boldsymbol{\sigma})$ is an even function, i.e. $H(\boldsymbol{\sigma}) = H(-\boldsymbol{\sigma})$, therefore it is expected that the probability distribution of the spin overlaps is symmetric, as is confirmed by the plots corresponding to the SK model in Fig.7,8, 9,10, unlike for the p-spin glass spherical model, as expected, since for the p-spin glass spherical model $H(\boldsymbol{\sigma})$ is an odd function, i.e. $H(\boldsymbol{\sigma}) = -H(-\boldsymbol{\sigma})$. The plots show that both models have non-trivial $P(q)$ and that as $N$ increases, the likelihood of orthogonal metastable states increases and parallel metastable states decreases. In addition, the plots are in accordance with G.Parisi's results for the SK model of $P(q)$ [8], that is as $N$ increases, $P(|q| = 1) \to 0$ which the plots also show is a property shared by the p-spin glass spherical model and as $N$ increases, for the SK model, the likelihood of $q = 0$ increases (also in accordance with results in [8]. However, in contrast, for the p-spin glass spherical model, the plots show that $q \approx -0.2$ is most probable, the likelihood of which increases as $N$ increases. Another distinctive feature between the two models, as shown by the plots is that $\mathcal{E}$ is an order of magnitude lower for the p-spin glass spherical model relative to the SK model, this result and the asymmetry of $P(q)$ for the p-spin glass spherical model could be a result of $M_N$ not being sufficiently large enough since a non-sufficiently large enough $M_N$ may result in the deviation of symmetry in $P(q)$.

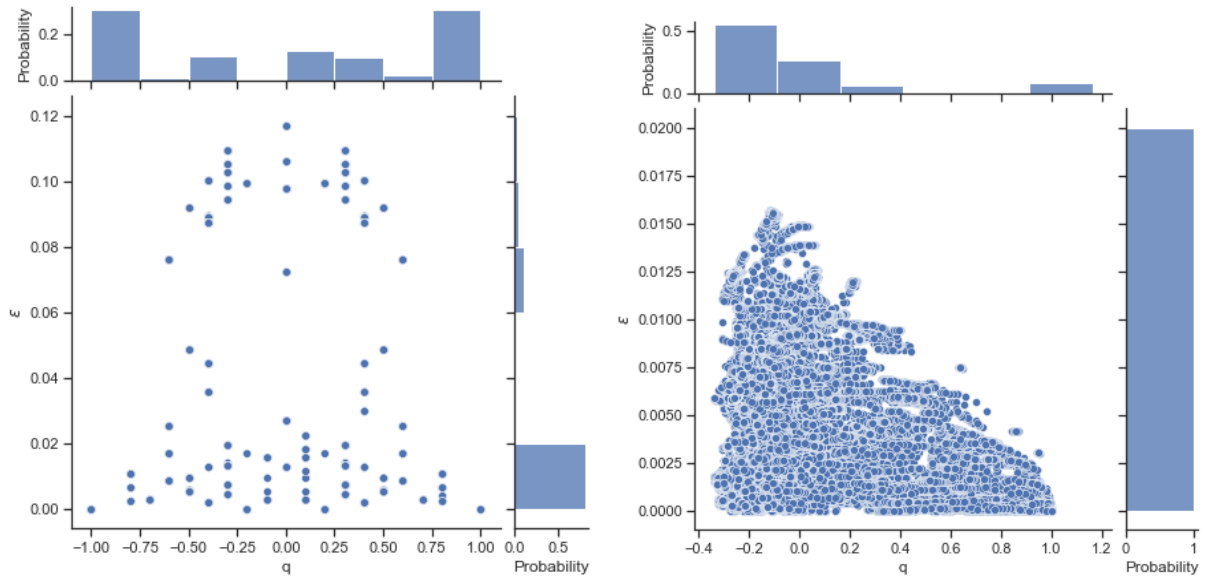


Figure 7: $\mathcal{E}$ as a function of $q$, with their marginal distributions provided, for $N = 20$ at $d_{0optimal}$. SK model (left): $t_{mcs} = 400, I_N = 500, M_N = 3$. P-spin glass spherical model (right): $t_{mcs} = 400, I_N = 500, M_N = 3$.

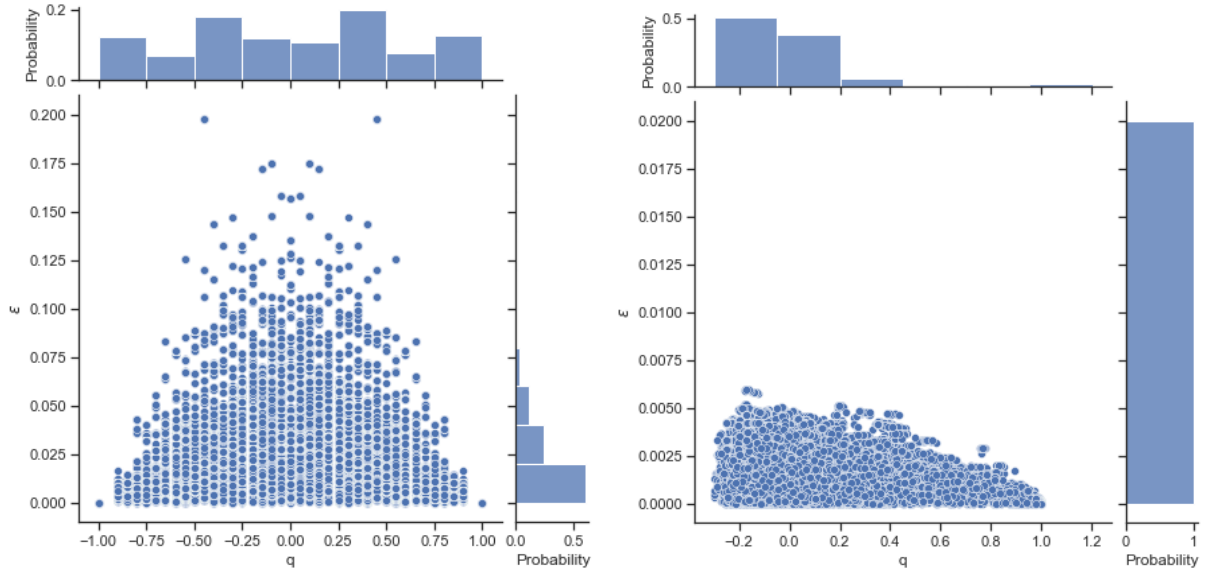


Figure 8: $\mathcal{E}$ as a function of $q$, with their marginal distributions provided, for $N = 40$ at $d_{0optimal}$. SK model (left): $t_{mcs} = 800, I_N = 1000, M_N = 5$. P-spin glass spherical model (right): $t_{mcs} = 200, I_N = 200, M_N = 3$.

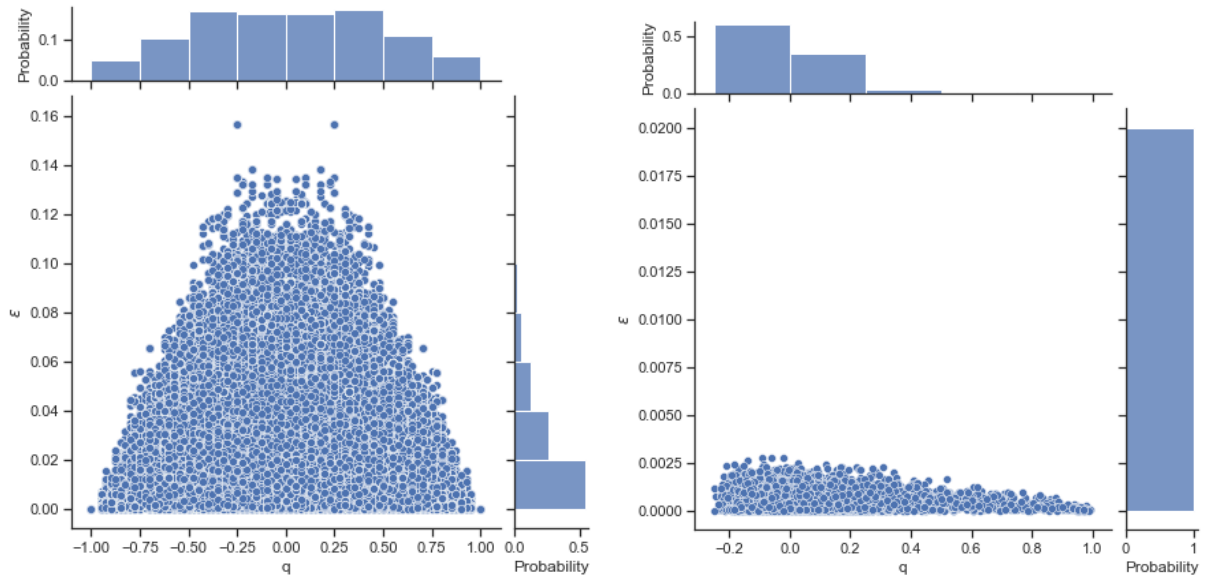


Figure 9: $\mathcal{E}$ as a function of $q$, with their marginal distributions provided, for $N = 80$ at $d_{0optimal}$. SK model (left): $t_{mcs} = 600, I_N = 800, M_N = 7$. P-spin glass spherical model (right): $t_{mcs} = 100, I_N = 100, M_N = 5$.

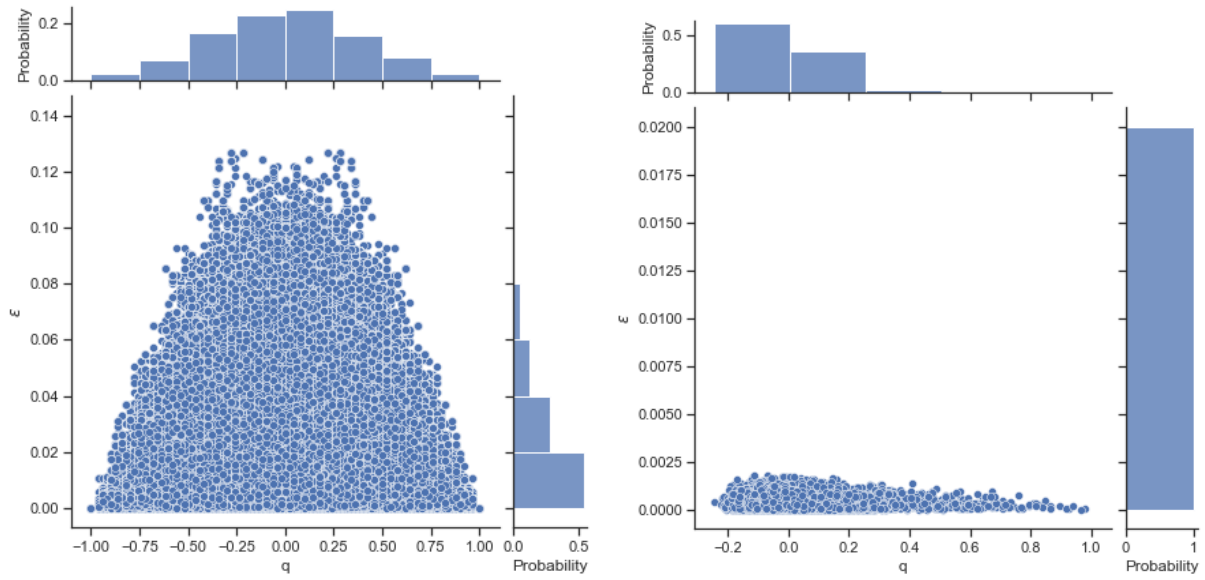


Figure 10: $\mathcal{E}$ as a function of $q$, with their marginal distributions provided, for $N = 100$ at $d_{0optimal}$. SK model (left): $N = 100, t_{mcs} = 500, I_N = 500, M_N = 8$. P-spin glass spherical model (right): $N = 100, t_{mcs} = 100, I_N = 100, M_N = 3$.

## 5 Phase-Space Diagnostics

As explained in [9], the OMCD algorithm is sensitive to properties of the phase-space of complex energy landscapes of the spin-glass systems. For instance, large moves are most likely to be accepted from the top of complex energy landscapes and large moves made deep within narrow valleys will most likely not be accepted as they would lead to moving higher up within the complex energy landscape. Such features can be displayed by tracking the number of accepted moves, $N_{acc}$ within each mcs that lead to a decrease in energy, $\Delta E < 0$ for every move-class size, see Fig.11 and 12. To provide a fair comparison of the number of accepted moves between the two models, $t_{mcs}$ is set equal for both models, which yields an equal number of total attempted moves for both models. In addition, $d_0 = d_{0optimal}$, $I_N >> M_N$ and $I_N$ is set sufficiently large enough as to remove any bias in results from initial conditions.

The plots in Fig.11 and 12 show that for both models, that (as expected) larger number of accepted moves tend to result in larger decreases in energy. In addition, the plots show that as $d$ decreases, the magnitude of energy decrease decreases too, which in conjunction with the entropy arguments given, confirms that the OMCD algorithm consistently hones in deeper within the valleys of the energy landscape and finds spin configurations closer to the bottom of the minima. However a distinctive feature between the two models is that when $d = 1$, the p-spin glass spherical model displays a dramatic difference of the number of accepted moves that is an order of magnitude larger relative to the SK model. This may be a consequence of the modification to the procedure of 'moves' made for the p-spin glass spherical model which allowed for a more rich exploration of the energy landscape.

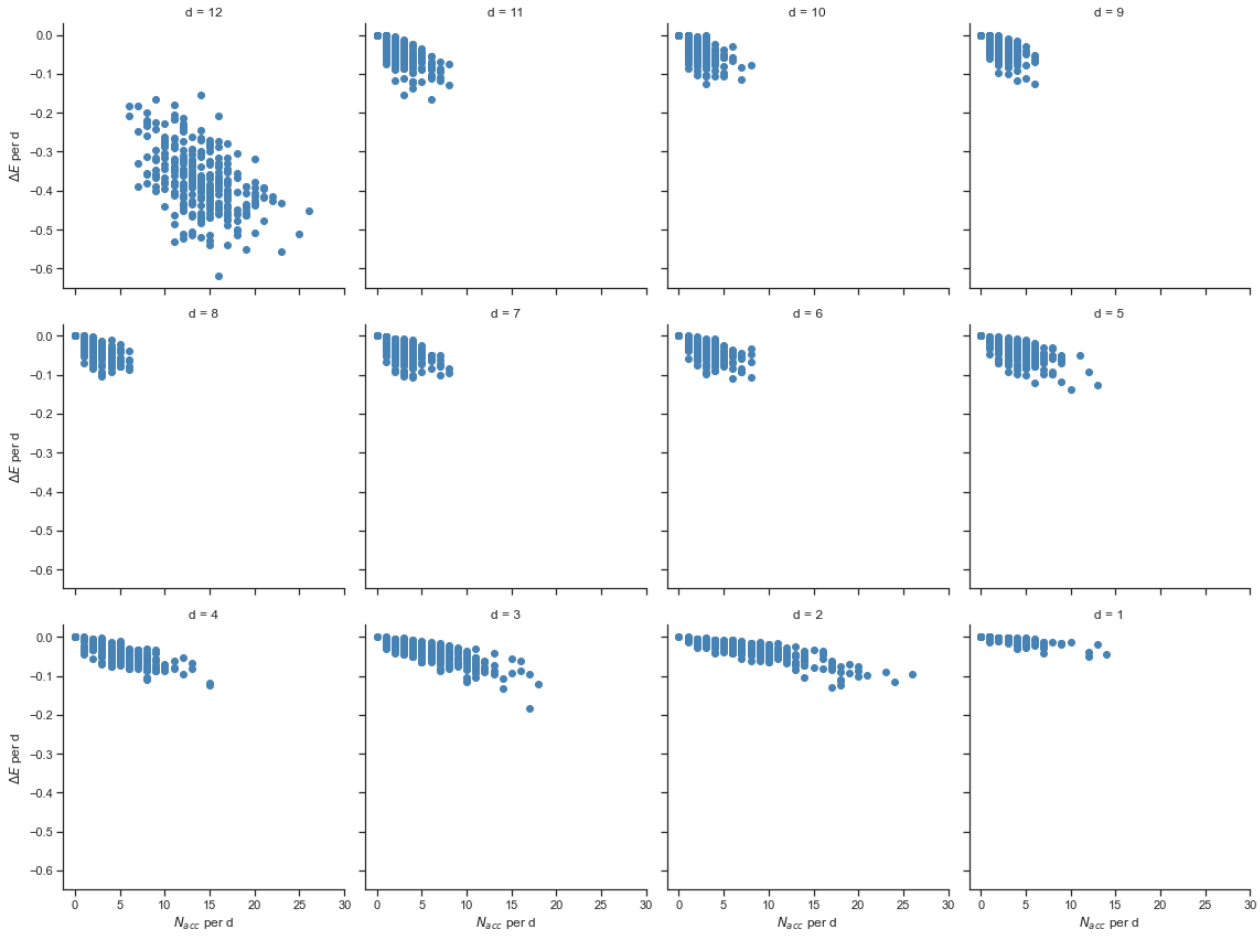


Figure 11: $\Delta E$ as a function of $N_{acc}$ for moves which only yield $\Delta E < 0$, displayed separately for each move class, for the SK model with $N = 100, t_{mcs} = 100, I_N = 100, M_N = 3$.

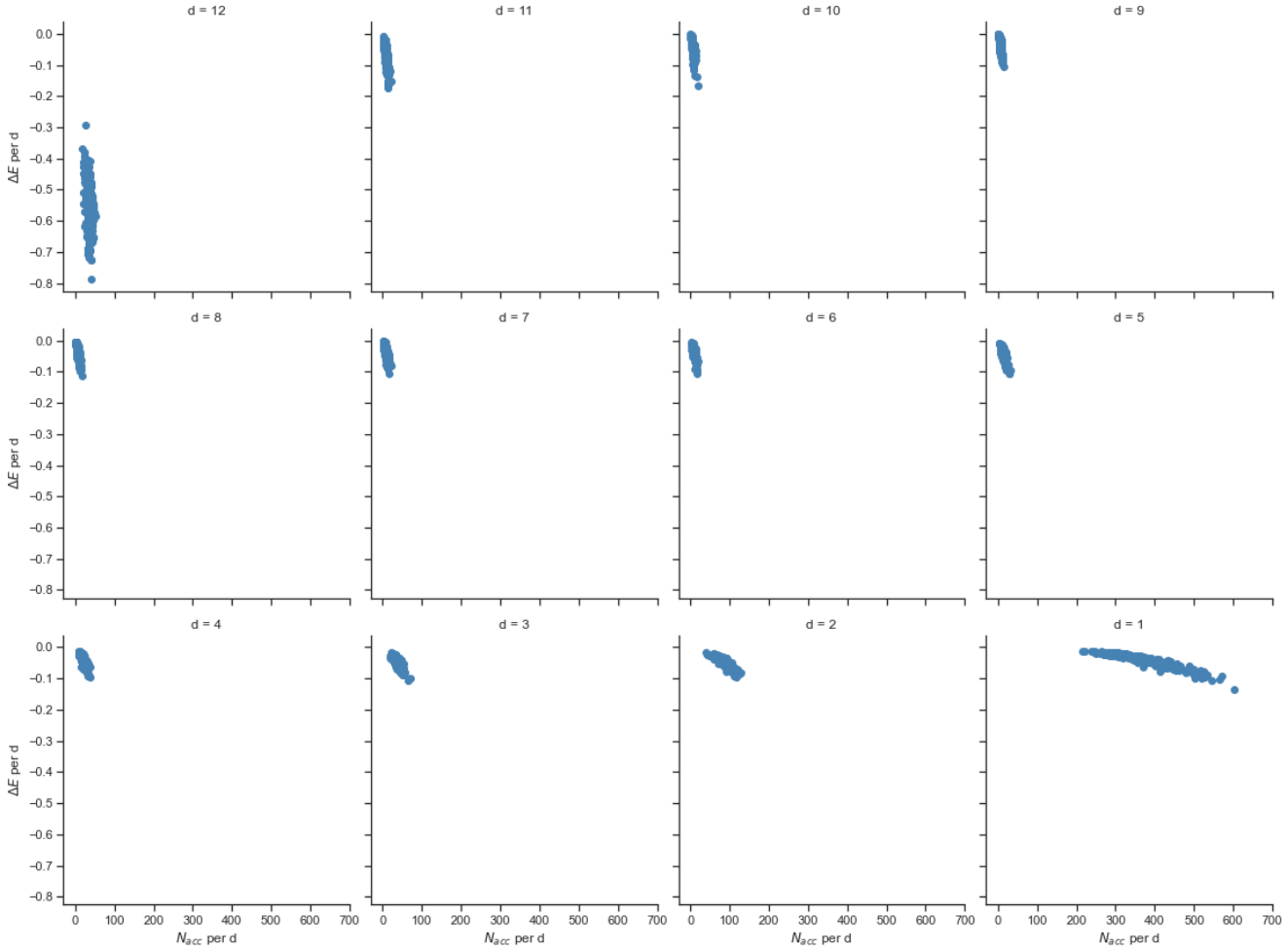


Figure 12: $\Delta E$ as a function of $N_{acc}$ for moves which only yield $\Delta E < 0$, displayed separately for each move class for the p-spin glass spherical model with $N = 100, t_{mcs} = 100, I_N = 100, M_N = 3$.

## 6 Summary and Discussion

In summary, this study has used the OMCD algorithm to present qualitative differences between the SK model and the p-spin glass spherical model, by first tackling the problem of finding ground state energies for both models, which for the infinite system size limit are approximated as -0.75946 and -1.14389, respectively. Thereafter the study provides insight into the nature of the metastable nature of the ground state energies at zero temperature for both models, where for the SK model the results display a symmetrical distribution of $P(q)$, and toward the infinite system size limit, the likelihood of orthogonal metastable states increases and the likelihood of parallel metastable states decreases. However for the p-spin glass model the results display that toward the infinite system size limit, the likelihood of parallel metastable states converges to zero and $q \approx -0.2$ being a lower bound and most probable. Due to the p-spin interaction, further work is required by considering much larger $M_N$ in order to verify the reliability of the obtained distribution of overlap between replicas at zero temperature for the p-spin glass model, it is expected that the distribution is symmetric for even values of $p$. More further work can be done to consider the effect of the initial conditions on the distribution of the overlap between replicas at zero temperature for both models, i.e. one may investigate for initial spin configurations with ferromagnetic or antiferromagnetic couplings being more probable. An obvious difference between the models at each

system size $N$ is that the set of spin configurations are distinct, where for the SK model, lie on the corners of the $N$-dimensional hyper-cube and for the p-spin glass spherical model, lie on the whole surface of the $N$-dimensional hyper-sphere. This may be the essential reason for the large difference in the number of accepted moves at $d = 1$ between the two models, hence comparing the SK model with Ising spins against the p-spin glass model with Ising spins, or comparing the SK model with spins given a spherical constraint against the p-spin glass spherical model may provide a more fair comparison.

## Acknowledgements

I would like to thank my supervisor Reimer Kühn for his helpful discussions and supervision over this project.

## References

[1] S F Edwards and P W Anderson. "Theory of spin glasses". In: *Journal of Physics F: Metal Physics* 5.5 (May 1975), pp. 965–974. DOI: 10.1088/0305-4608/5/5/017. URL: https://doi.org/10.1088/0305-4608/5/5/017.

[2] David Sherrington and Scott Kirkpatrick. "Solvable Model of a Spin-Glass". In: *Physical Review Letters* 35 (Dec. 1975), pp. 1792+. DOI: 10.1103/PhysRevLett.35.1792.

[3] G Parisi. "A sequence of approximated solutions to the S-K model for spin glasses". In: *Journal of Physics A: Mathematical and General* 13.4 (Apr. 1980), pp. L115–L121. DOI: 10.1088/0305-4470/13/4/009. URL: https://doi.org/10.1088/0305-4470/13/4/009.

[4] Daniel J Amit, Hanoch Gutfreund, and Haim Sompolinsky. "Storing infinite numbers of patterns in a spin-glass model of neural networks". In: *Physical Review Letters* 55.14 (1985), p. 1530.

[5] Joseph D Bryngelson and Peter G Wolynes. "Spin glasses and the statistical mechanics of protein folding." In: *Proceedings of the National Academy of sciences* 84.21 (1987), pp. 7524–7528.

[6] J. Kurchan, G.Parisi, and M.A. Virasoro. "Barriers and metastable states as saddle points in the replica approach". In: *J. Phys. I France* 3.8 (1993), pp. 1819–1838. DOI: 10.1051/jp1:1993217. URL: https://doi.org/10.1051/jp1:1993217.

[7] Scott Kirkpatrick and Gregory B Sorkin. "Simulated annealing". In: (1995).

[8] Giorgio Parisi. *On the Statistical Properties of the Large Time Zero Temperature Dynamics of the SK Model*. 1995. DOI: 10.48550/ARXIV.COND-MAT/9501045. URL: https://arxiv.org/abs/cond-mat/9501045.

[9] Reimer Kühn, Yu-Cheng Lin, and Gerhard Pöppel. "Optimization by Move–Class Deflation". In: *arXiv preprint cond-mat/9805137* (1998).

[10] Daniel L Stein. "Spin glasses: still complex after all these years?" In: *Decoherence and Entropy in Complex Systems*. Springer, 2004, pp. 349–361.

[11] Jean-Philippe Bouchaud. "The (unfortunate) complexity of the economy". In: *Physics World* 22.04 (2009), p. 28.

[12] Marco Baity-Jesi et al. "Comparing dynamics: Deep neural networks versus glassy systems". In: *International Conference on Machine Learning*. PMLR. 2018, pp. 314–323.

# 7 Self Assessment

In this study I have explored the problem of tackling the ground state energies for the SK model and the p-spin glass spherical model. I have correctly implemented the OMCD algorithm using the Python programming language. A challenge I had faced was to efficiently calculate the Hamiltonian for the p-spin glass spherical model, since for larger systems, the number of p-spin interactions was computationally expensive, and it is for this reason that the number of samples taken for the p-spin glass spherical model was lower relative to the SK model, however within the time constraints given I have tried my best to produce statistically reliable results. In addition, I have tried my best to ensure correct spelling, use of mathematical notation and the readability of the thesis to be good. I have correctly summarised the general outline of the study in the abstract, provided a sufficient introduction to the concepts covered in the thesis by first providing intuition for the characteristic properties of spin-glass systems (frustration and quenched disorder) and also mentioned a suitable range of relevant background material of the models and a brief mention of the numerical attempts at solving them, and then ending with mention of the direction of the study. The figures provided are of a suitable size and thus clear to read, with all relevant information provided in the captions. The conclusion provided had succinctly summarised the results and includes a critical discussion of the results, as well as some further work that could be done. Lastly, I had provided references whenever any information obtained outside of the lecture module content was given, and the list of all references are provided at the end of the thesis.